Ubiquitylation by Trim32 causes coupled loss of desmin, Z-bands, and thin filaments in muscle atrophy

Shenhav Cohen, Bo Zhai, Steven P. Gygi, and Alfred L. Goldberg

Department of Cell Biology, Harvard Medical School, Boston, MA 02115

During muscle atrophy, myofibrillar proteins are degraded in an ordered process in which MuRF1 catalyzes ubiquitylation of thick filament components (Cohen et al. 2009. *J. Cell Biol.* http://dx.doi.org/10.1083/jcb.200901052). Here, we show that another ubiquitin ligase, Trim32, ubiquitylates thin filament (actin, tropomyosin, troponins) and Z-band (α-actinin) components and promotes their degradation. Down-regulation of Trim32 during fasting reduced fiber atrophy and the rapid loss of thin filaments. Desmin filaments were proposed to maintain the integrity of thin filaments. Accordingly, we find that the rapid destruction of thin filament proteins upon fasting was accompanied by increased phosphorylation of desmin filaments, which promoted desmin ubiquitylation by Trim32 and degradation. Reducing Trim32 levels prevented the loss of both desmin and thin filament proteins. Furthermore, overexpression of an inhibitor of desmin polymerization induced disassembly of desmin filaments and destruction of thin filament components. Thus, during fasting, desmin phosphorylation increases and enhances Trim32-mediated degradation of the desmin cytoskeleton, which appears to facilitate the breakdown of Z-bands and thin filaments.

Introduction

Atrophy of skeletal muscle occurs with disuse or denervation and systemically in fasting and disease states, including sepsis, cancer cachexia, and renal and cardiac failure (Jackman and Kandarian, 2004; Lecker et al., 2006). In these conditions, the rapid loss of muscle mass results largely from the accelerated degradation of myofibrils, which comprise the majority of muscle proteins. Myofibrillar proteins are degraded primarily by the ubiquitin–proteasome system (Solomon and Goldberg, 1996). Two ubiquitin ligases, Muscle RING finger 1 (MuRF1) and Atrogin-1/MAFbx, are induced in all types of atrophy (Gomes et al., 2001), and the loss of either enzyme reduces muscle wasting (Bodine et al., 2001). In addition, autophagy is stimulated and accelerates the breakdown of organelles and soluble proteins (Mammucari et al., 2007; Zhao et al., 2008).

Because myofibrillar proteins are highly organized into filaments and sarcomeres, their disassembly and degradation must be a complex, highly selective process, especially because muscles continue to function even during rapid atrophy (e.g., in fasting). We recently discovered that contractile proteins are lost in an ordered fashion during denervation atrophy (Cohen et al., 2009). Certain regulatory proteins that stabilize the thick filament (myosin-binding protein C and light chains 1 and 2) are lost first by a MuRF1-dependent mechanism after which myosin heavy chain is ubiquitylated by this enzyme and degraded (Clarke et al., 2007; Fielitz et al., 2007; Cohen et al., 2009). However, thin filament (i.e., actin, tropomyosin, troponins) and Z-band (α-actinin) components are lost by a mechanism not requiring MuRF1 (Cohen et al., 2009). We show here that their degradation requires a distinct RING finger ubiquitin ligase, Trim32 (tripartite motif–containing protein 32).

Trim32 belongs to the large family of proteins containing a tripartite motif (RING; B-box; coiled-coil), but in addition, it has six NHL repeats that may bind substrates (Slack and Ruvkun, 1998; Frosk et al., 2002). Unlike MuRF1 or Atrogin1, Trim32 is expressed throughout the body. In humans, mutations at the third NHL repeat cause limb girdle muscular dystrophy 2H (Frosk et al., 2002), but the effects of these mutations on its function are unclear. Recently, Spencer and colleagues described a Trim32 knockout mouse that exhibits a mild myopathy and a decrease in brain neurofilaments (Kudryashova et al., 2011).

Correspondence to Alfred L. Goldberg: alfred_goldberg@hms.harvard.edu

Abbreviations used in this paper: DN, dominant negative; IF, intermediate filament; LGMD-2H, limb girdle muscular dystrophy 2H; MyBP-C, myosin-binding protein-C; MyHC, myosin heavy chain; MyLC2, myosin light chain 2; MuRF1, muscle RING-finger 1; p97/VCP, P97/vasolin-containing protein; PP1, protein phosphatase 1; TA, tibialis anterior; Tm, Tropomyosin; TnI, Troponin I; TnT, Troponin T; Trim32, tripartite motif-containing protein 32.

The Rockefeller University Press $30.00
J. Cell Biol. Vol. 198 No. 4 575–589
www.jcb.org/cgi/doi/10.1083/jcb.201110067

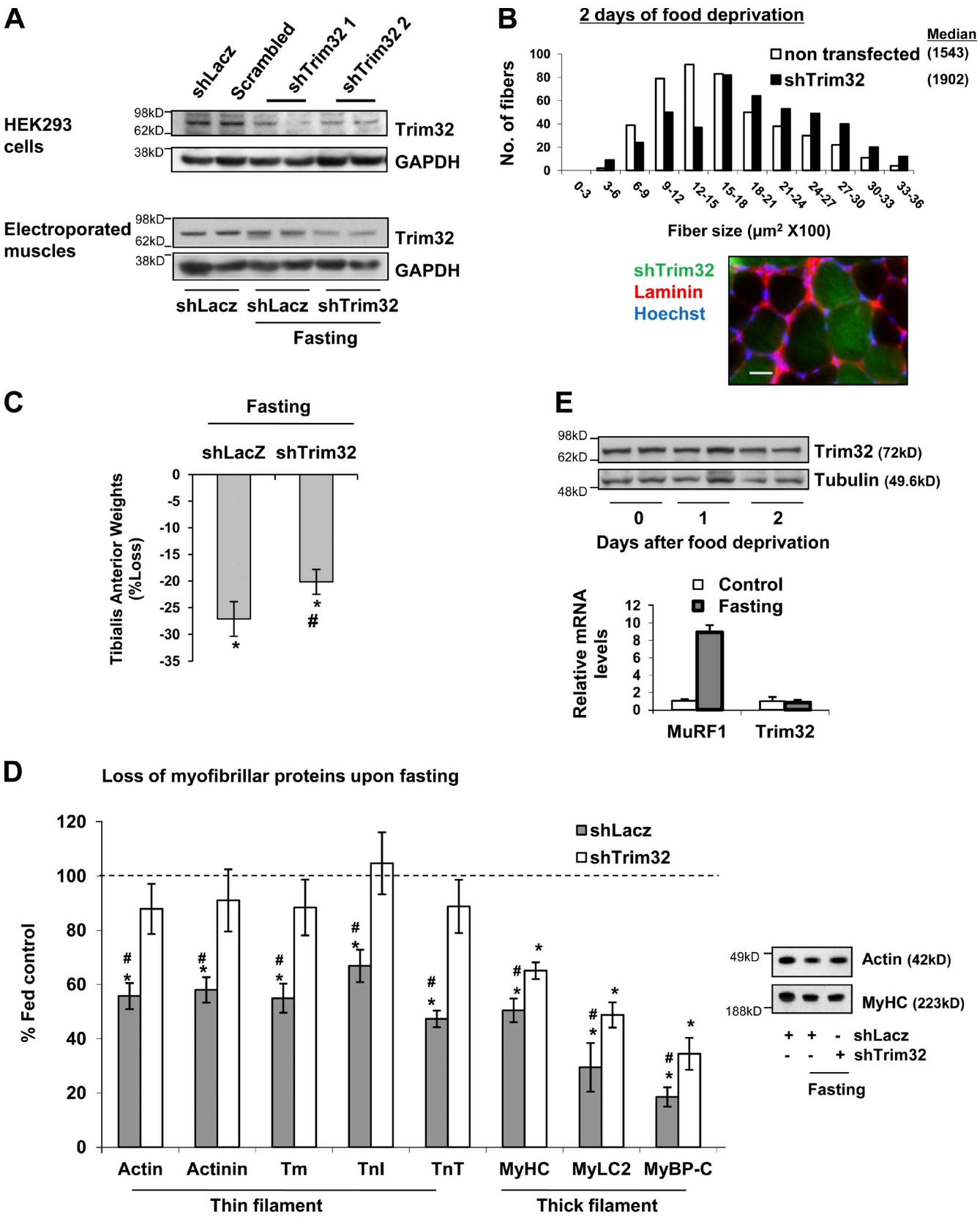

Figure 1. **Trim32 is required for muscle atrophy induced by fasting.** TA muscles were electroporated with shRNA vectors against Trim32 (shTrim32) or Lacz (shLacz), and 4 d later mice were deprived of food for 2 d. In fed mice, muscles were dissected 6 d after electroporation. Electroporation of shLacz into fibers of fasted or fed control mice did not affect fiber size (Sandri et al., 2004). (A) shRNA-mediated knockdown of Trim32 in HEK293 cells (top) and muscles from fasted animals (bottom). Soluble extracts were analyzed by immunoblotting. (B) Down-regulation of Trim32 in muscles from fasted

They also reported that Trim32 content increases during atrophy induced by hind-limb suspension and that it can monoubiquitylate actin (Kudryashova et al., 2009). Although Trim32 seems to have important roles in muscle, its precise functions are not yet known. We demonstrate here that during fasting-induced atrophy, Trim32 catalyzes the loss of thin filament and Z-band components through effects on the key cytoskeletal protein, desmin.

In muscle, desmin forms intermediate filaments (IFs) that are localized between adjacent myofibrils, linking them laterally to the Z-lines, and between myofibrils and the sarcolemma, mitochondria, and nuclear membrane (Lazarides and Hubbard, 1976; Lazarides, 1978). Mice lacking desmin exhibit misaligned sarcomeres and disorganized myofibrils in skeletal and cardiac muscle (Milner et al., 1996). Missense mutations in desmin cause a cardiomyopathy characterized by disarrayed myofibrils, and expression of this mutant desmin in cardiomyocytes displaces endogenous desmin from the Z-lines and perturbs actin filament architecture (Conover et al., 2009). These findings highlight the importance of desmin IFs for the integrity of myofibrils. The present studies demonstrate that desmin IFs are phosphorylated, disassembled, and degraded upon fasting, that these events facilitate thin filament breakdown, and that Trim32 is critical in destruction of both structures.

Desmin IFs depolymerize upon phosphorylation (Geisler and Weber, 1988). Desmin is composed of an N-terminal head domain, a C-terminal tail domain, and a central conserved α-helical coiled-coil rod (Geisler and Weber, 1982). The head domain is important for filament stability and polymerization, as its removal prevents polymerization (Kaufmann et al., 1985), and phosphorylation of serine residues in this domain promotes IF depolymerization (Inagaki et al., 1987). We show here that during atrophy, phosphorylation in this domain promotes ubiquitylation by Trim32 and destruction of desmin filaments, whose disassembly reduces the stability of thin filaments.

In this study, we investigated: (i) whether Trim32 contributes to muscle atrophy and thin filament loss upon fasting, and (ii) what are Trim32's substrates in muscle? The finding that desmin is a substrate led us to ask (iii) whether this IF protein is also lost in atrophy, (iv) whether Trim32 is responsible for degradation of desmin filaments and the loss of the Z-band component, α-actinin, during atrophy, and (v) whether disassembly of the desmin cytoskeleton is linked to the loss of thin filament components.

Results

Trim32 is required for muscle atrophy upon fasting

The ubiquitin ligase MuRF1 promotes degradation of thick filaments, but is not required for the loss of thin filaments during denervation atrophy (Cohen et al., 2009). Because the RING E3, Trim32, is induced upon unloading and can ubiquitylate actin in vitro (Kudryashova et al., 2005), we tested whether it is essential for the rapid muscle wasting and the loss of thin filament proteins. We suppressed Trim32 expression by electroporation into mouse tibialis anterior (TA) of plasmids encoding GFP (to identify the transfected fibers) and shRNA vectors (shTrim32), which efficiently reduced Trim32 content in 293 cells (Fig. 1 A, top). 4 d later, when there was no change in muscle size (Fig. S1 A), we deprived the mice of food for 2 d and analyzed the effects on fiber size and muscle weight. In the transfected muscles, the shTrim32 decreased Trim32 protein below the levels in control fibers electroporated with shRNA to Lacz (shLacz; Fig. 1 A, bottom), but the actual decrease in Trim32 level in these fibers must be even greater because only 70% of the fibers were transfected. By 2 d of fasting, there was a 27% decrease in the mean weight of the control TA muscles below levels in fed mice (Fig. 1 C). The reduction in Trim32 clearly attenuated this wasting, even though ∼30% of the fibers were not transfected with the shTrim32 (Fig. 1 C). Furthermore, the mean cross-sectional area of 500 fibers expressing shTrim32 was much greater than that of 500 nontransfected fibers in the same muscle (Fig. 1 B and Fig. S1 B). Thus, Trim32 function is clearly important for the atrophy induced by fasting.

Trim32 is necessary for the loss of thin filaments

To learn if Trim32 catalyzes the loss of thin filament proteins from the myofibril, we analyzed the effect of Trim32 down-regulation on the total content of thin filament components upon fasting. Equal amounts of isolated myofibrils from muscles transfected with shTrim32 or shLacz were analyzed by SDS-PAGE and Coomassie blue staining, and the intensity of specific protein bands was measured by densitometry. Previously, we identified these different protein bands by mass spectrometry (Cohen et al., 2009; Fig. S1 C). To determine the absolute content of each myofibrillar protein in the muscle, the density of each band was multiplied by the total amount of myofibrillar proteins per muscle and then by the total muscle weight (see Materials and

mice reduces fiber atrophy. Measurement of cross-sectional area of 500 fibers transfected with shTrim32 (and expressing GFP; black bars) vs. 500 nontransfected fibers (open bars) in the same muscle. Data acquired from six mice. Green fibers express shTrim32 and laminin staining in red. Bar, 75 µM. (C) Down-regulation of Trim32 attenuates the loss of muscle mass during fasting. shTrim32 was delivered to more than 70% of muscle fibers. Mean weights of electroporated muscles are plotted as the percent weight loss. $n = 6$. *, $P < 0.001$ vs. fed control; #, $P < 0.05$ vs. shLacz (see also data in Fig. 5 B). (D) Down-regulation of Trim32 prevents the loss of thin and slightly reduced the loss of thick filament components during fasting. Left: isolated myofibrils from shLacz- (shaded) or shTrim32-expressing muscles (open) were analyzed by SDS-PAGE and Coomassie blue staining. To obtain the absolute content of each myofibrillar protein, densitometric measurement of specific bands was performed, and the values were multiplied by the total amount of myofibrils per muscle and then by muscle weight. The content of each myofibrillar protein is presented as the percentage of fed control. $n = 6$. *, $P < 0.05$ vs. fed control; #, $P < 0.05$ vs. shTrim32. Right: equal fractions of myofibrils were analyzed by Western blot using anti-actin and anti-MyHC. (E) Trim32 is not induced upon fasting. Top: soluble fraction of muscles, 1 or 2 d after food deprivation, were analyzed by SDS-PAGE and immunoblotting. Bottom: quantitative RT-PCR of mRNA preparations from atrophying and control muscles using primers for MuRF1 and Trim32. Data are plotted as the mean fold change relative to control. $n = 6$.

Table 1. **Trim32 binds thin filament and Z-band components in the muscle homogenate**

Protein name	Gene	No. of unique peptides (found initially)	Precipitated from normal muscle with pure Trim32	Ubiquitylated after the addition of E1, E2, and ATP
α-Actin	Acta1	5	+	+
α-Actinin	Actn3	1	+	+
Tropomyosin 1 alpha chain	Tpm1	1	+	+
Desmin	Des	1	+	+
Myosin regulatory light chain	Mylpf	1	+	

Trim32-bound proteins were precipitated together with Trim32 from the soluble fraction of TA and identified by mass spectrometry. When a subsequent in vitro ubiquitylation reaction was carried out, mass spectrometry analysis identified actin, α-actinin, Tm, and desmin as ubiquitylated species.

methods). The total content of each myofibrillar component in the atrophying muscle was then expressed as the percentage of this protein's content in the corresponding muscles in the fed mice (Fig. 1 D). The content of each major thin filament component, actin, tropomyosin (Tm), troponin I (TnI), and troponin T (TnT), and the Z-band protein α-actinin decreased by more than 40% in the contralateral atrophying muscles (expressing shLacz) below levels in control muscles from fed animals (Fig. 1 D). This loss of myofibrillar proteins exceeded the relative loss of muscle mass; thus, these components decreased in fasting to a greater extent than the bulk of cell proteins and especially the soluble proteins.

Trim32 down-regulation by transfection of shRNA blocked the loss of thin filament proteins and α-actinin, whose content no longer differed significantly from that in muscles of fed controls. By contrast, the shTrim32 only slightly reduced the loss of thick filament components, myosin heavy (MyHC) and light (MyLC2) chains and binding protein C (MyBP-C), which decreased by more than 40% (Fig. 1 D, Table S1). This selective sparing of thin filament components was further supported by Western blot analysis of actin and MyHC in equal fractions of myofibrils from transfected muscles (Fig. 1 D, right). Thus, upon fasting, Trim32 plays a critical role in the rapid atrophy, especially in the breakdown of thin filament components. In fact, the sparing of these proteins by shTrim32 in Fig. 1 D must underestimate the protective effects of Trim32 down-regulation because only about half the fibers were transfected. It is noteworthy that neither Trim32 protein nor mRNA increased upon fasting (Fig. 1 E), although this enzyme is clearly essential for the loss of muscle mass (Fig. 1, B and C; and see Fig. 5 B).

Actin and other myofibrillar components are substrates for Trim32

Because Trim32 is required for the loss of thin filament components, we investigated whether any muscle proteins are direct substrates for Trim32 using a similar approach as we used to identify MuRF1's substrates (Cohen et al., 2009). To isolate proteins having a high affinity for Trim32, soluble extracts of TA were cleared with immobilized GST and then incubated with immobilized GST-Trim32. The resulting precipitates were washed extensively with buffer containing 500 mM NaCl to remove nonspecific or weakly associated proteins. The Trim32-bound proteins were identified by mass spectrometry, which revealed several groups of proteins, including the major thin filament components actin and Tm, the Z-line component α-actinin, the cytoskeletal protein desmin (Table 1; although only a few unique peptides were identified for Tm, α-actinin, and desmin), and the thick filament component MyLC2. It is noteworthy that these myofibrillar and cytoskeletal components, though primarily insoluble, were present and bound to Trim32 in the soluble fraction (see also Fig. 2 B).

To determine whether these proteins are substrates for Trim32, we added the washed Trim32-bound precipitates to a ubiquitylation reaction containing E1, UbcH5 as the E2, ATP, and 6His-ubiquitin. The 6His-tagged ubiquitylated proteins were purified with a Nickel column and analyzed by mass spectrometry. Actin, α-actinin, Tm, and desmin were all found to be ubiquitylated by Trim32 (Table 1).

To confirm these findings by an independent approach, we assayed in vitro ubiquitylation of pure actin and Tm by Trim32 with either UbcH5 or UbcH13/Uev1 as the E2. Although Spencer and colleagues reported that Trim32 can only monoubiquitylate soluble actin (Kudryashova et al., 2005), we found that Trim32 polyubiquitylated soluble actin and also actin within purified myofibrils (Fig. 2 A). In addition, Trim32 polyubiquitylated Tm, as well as the thick filament component MyLC2, though to a lesser extent than actin (Fig. 2 A). However, under these conditions, i.e., with the undissociated myofibrils, α-actinin, Tm, MyLC2, and MyHC were not ubiquitylated by Trim32 (not depicted). Thus, Trim32 ubiquitylates pure actin preferentially, and in the intact myofibril only actin is ubiquitylated. Thus, actin is Trim32's preferred substrate, and the small effect of Trim32 down-regulation on levels of thick filaments (Fig. 1 D) is probably indirect.

Surprisingly, these studies also demonstrate that soluble pools of Tm, α-actinin, actin, MyHC, and MyLC2 exist in muscle. The fraction soluble at 3,000 *g* contains contractile proteins that seemed to have been released during myofibrillar breakdown. Western blot analysis showed that these soluble pools of myofibrillar proteins were smaller during fasting, but not if Trim32 was inhibited by electroporation of a dominant negative (Trim32-DN), which lacks the catalytic ring finger domain and thus can bind substrates but cannot ubiquitylate them (Fig. 2 B; Kano et al., 2008). These results strongly suggest that these proteins are substrates for Trim32 in vivo, although Trim32 can also ubiquitylate myofibrillar actin (Fig. 2 A). Because muscle protein synthesis falls during fasting (Li and Goldberg, 1976), the decrease in soluble fraction of Tm, α-actinin, actin, MyHC, and MyLC2 upon fasting probably represents enhanced dissociation of myofibrillar constituents and their accelerated destruction by a Trim32- or MuRF1-dependent mechanism.

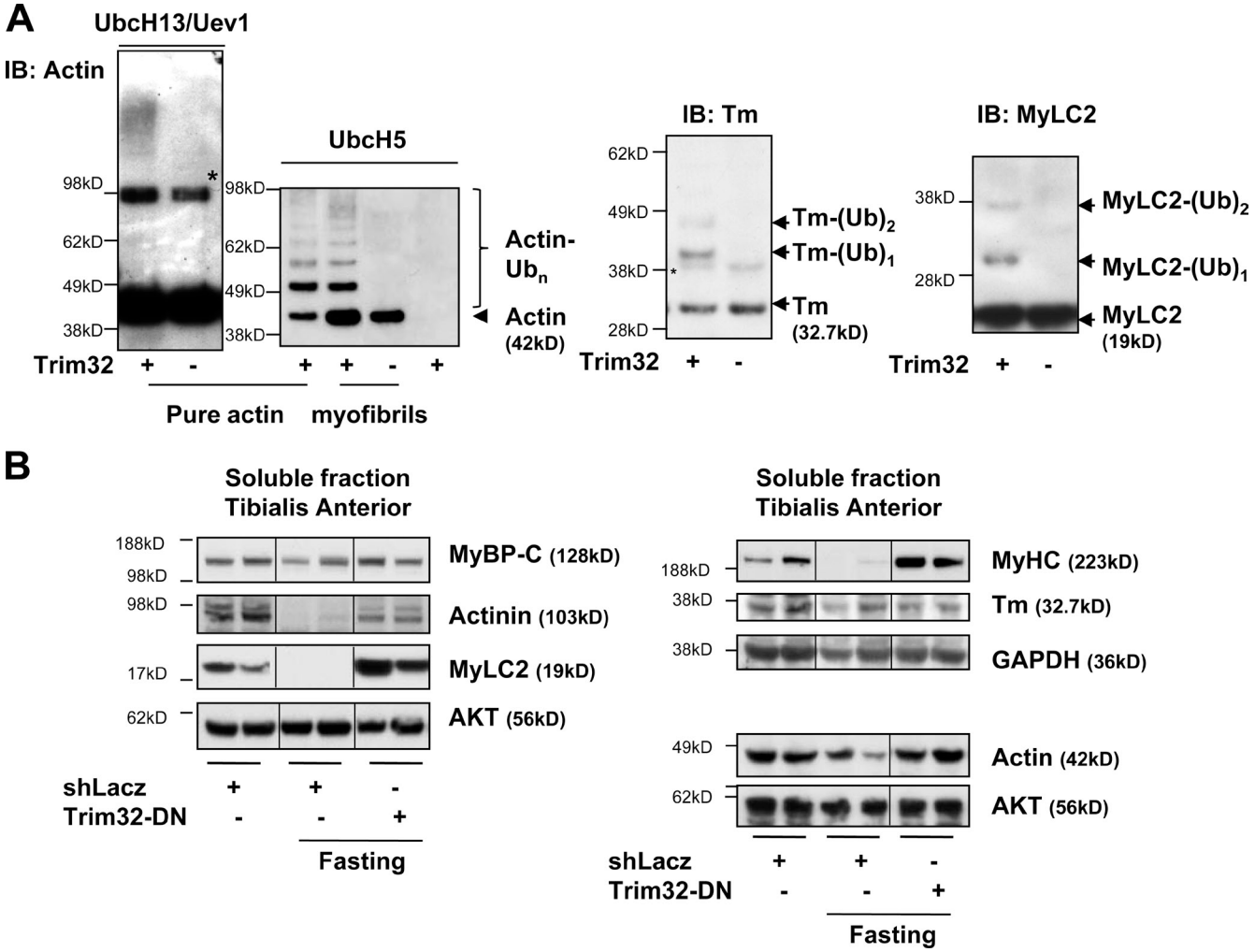

Figure 2. **Actin and other myofibrillar proteins are substrates for Trim32.** (A) In vitro ubiquitylation of actin, tropomyosin (Tm), and MyLC by Trim32 was analyzed by immunoblotting with specific antibodies. Asterisk represents nonspecific bands. (B) Muscle extracts contain soluble forms of actin, α-actinin, Tm, MyHC, MyLC2, and MyBP-C, whose loss requires Trim32 during fasting. Soluble fractions of normal and atrophying muscles expressing shLacz or shTrim32 were analyzed by SDS-PAGE, and immunoblot analysis using antibodies against the indicated proteins. Each lane is a separate muscle, and representative bands were chosen based on similar atrophy rates in transfected muscles.

During atrophy, desmin filaments are phosphorylated, solubilized, and degraded

Desmin IFs compose the primary cytoskeletal network in muscle and are important in maintaining myofibrillar stability and alignment (Milner et al., 1996; Li et al., 1997). Phosphorylation of desmin filaments in vitro promotes their disassembly (Geisler and Weber, 1988) and in cardiomyocytes leads to myofibrillar disarray (Huang et al., 2002). Also, expression of a mutant desmin in cardiomyocytes perturbs actin filament architecture (Conover et al., 2009). These findings suggest that desmin filaments are important for thin filament organization and raise the possibility that desmin phosphorylation may trigger myofibrillar dissociation during atrophy. Because desmin in the soluble fraction bound to and was ubiquitylated by Trim32 (Table 1), we tested whether its filaments are phosphorylated, disassembled, and degraded during fasting in a Trim32-dependent fashion.

To learn if desmin is lost upon fasting, we performed immunofluorescence staining of longitudinal sections of TA from fed and fasted mice. Desmin has been reported to be confined to Z-lines (Conover et al., 2009), and accordingly a striated pattern of desmin IFs was observed in muscles from fed mice (Fig. 3 A). However, in muscles from fasted mice, the staining intensity of desmin was dramatically reduced (Fig. 3 A). These findings indicate a marked loss of desmin upon fasting, as was reported in denervated human muscles (Helliwell et al., 1989; Boudriau et al., 1996).

To determine if desmin is phosphorylated in muscles of fasted mice, we analyzed the 3,000-*g* pellet of homogenates of TA muscles expressing shTrim32. Reducing Trim32 content should result in an accumulation of its substrates and should facilitate their identification. By isoelectric focusing 2D gel electrophoresis and Coomassie blue staining, four spots were observed at the molecular weight of desmin (~53 kD; Fig. 4 A) that were identified by tandem mass spectrometry as the IF protein vimentin, and three species of desmin, which differed in isoelectric point due to phosphorylation at Ser-28, Ser-32, and Ser-68 (Fig. 4 A). Desmin phosphorylation was confirmed by immunoblot analysis of the 2D gel with antibodies against desmin

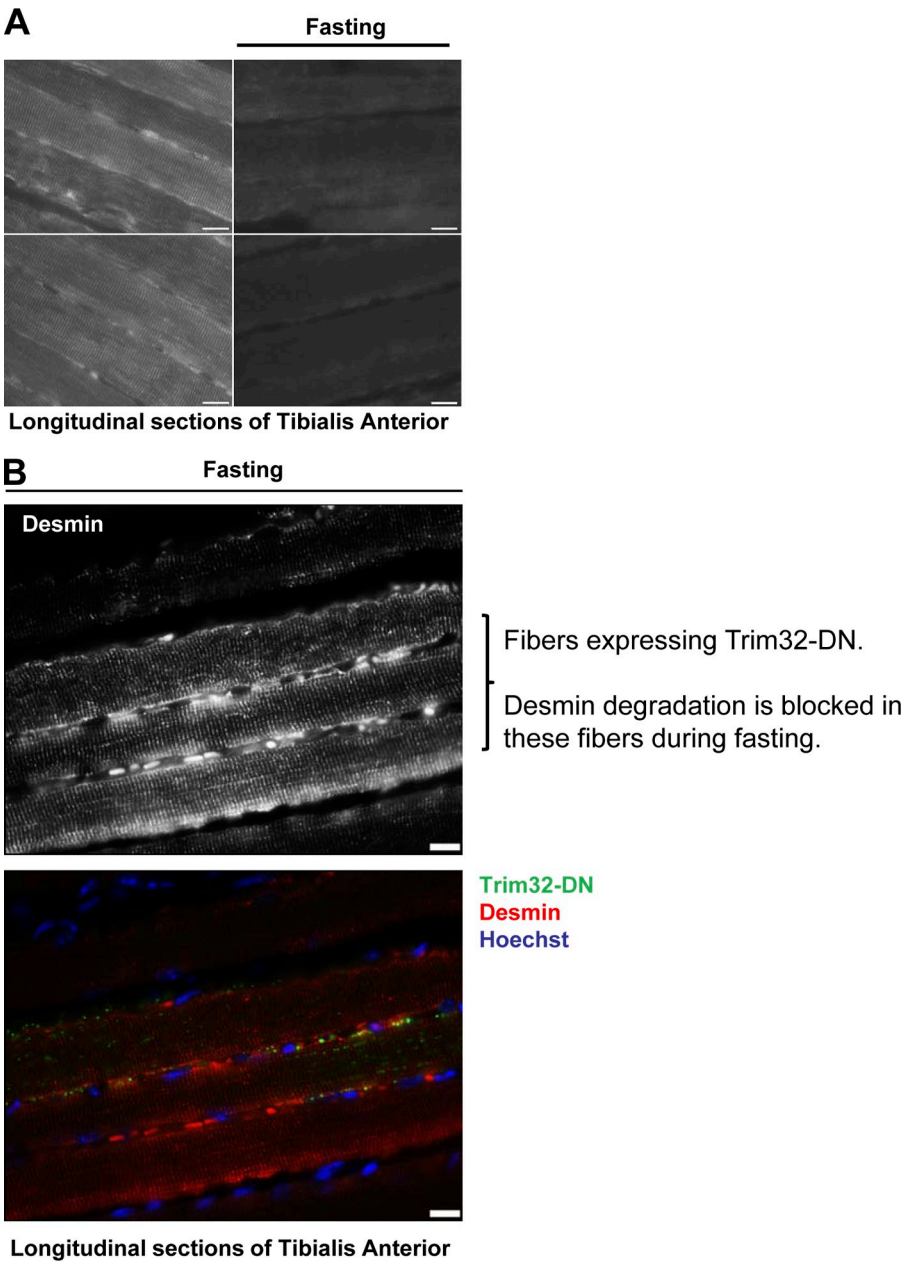

Figure 3. **Desmin is lost during atrophy induced by fasting.** (A) Paraffin-embedded longitudinal sections of TA muscle from fed mice and ones deprived of food (2 d) were stained with an antibody against desmin. Bar, 25 µM. (B) During fasting, depolymerization of desmin filaments is prevented in muscle fibers expressing Trim32-DN. Paraffin-embedded longitudinal sections of TA muscles expressing Trim32-DN (green) from fasted mice were stained with an antibody against desmin (red). Desmin filaments are degraded in two fibers, which do not express Trim32-DN, at the two opposite edges of the image. Expression of Trim32-DN in the three fibers in the center of the image markedly attenuated the loss of desmin. Bar, 25 µM.

and phospho-serine (Fig. 4 A). These residues are located within desmin's head domain, and phosphorylation in this region was reported to trigger depolymerization of desmin filaments (Inagaki et al., 1987), as we show below also occurs during fasting (see Fig. 4).

We then tested if upon fasting, desmin filaments are phosphorylated before their degradation. We purified desmin filaments from muscles of fed and fasted mice by treating the myofibrillar fraction with 0.6 M KCl for 10 min to extract myofibrillar proteins, but not desmin IFs, which were not solubilized by these conditions (Fig. S2). SDS-PAGE and immunoblotting with anti–phospho-serine revealed phosphorylated desmin filaments in the control muscles, which decreased in amount during fasting (Fig. 4 B). The total amount of desmin filaments in the muscles was also reduced during this rapid atrophy (Fig. 4 B), strongly suggesting increased degradation of these cytoskeletal proteins. In these muscles there was also a reduction in the amount of phosphorylated desmin in the 3,000-*g* supernatant (Fig. 4, B and C), which implies enhanced disassembly and degradation of the phosphorylated desmin filaments during fasting that we demonstrate is dependent on Trim32 (see next paragraph).

Trim32 promotes disassembly and destruction of desmin filaments

To determine if Trim32 is required for desmin loss, we analyzed the reduction in the amount of desmin filaments upon fasting after electroporation of shTrim32. Down-regulation of Trim32 blocked the decrease in desmin upon fasting (Fig. 4 B); instead, desmin accumulated as insoluble phosphorylated filaments and also in the soluble fraction (Fig. 4 B). Similar results were obtained when we electroporated Trim32-DN (Fig. 3 B, unpublished data). In fact, the content of phosphorylated

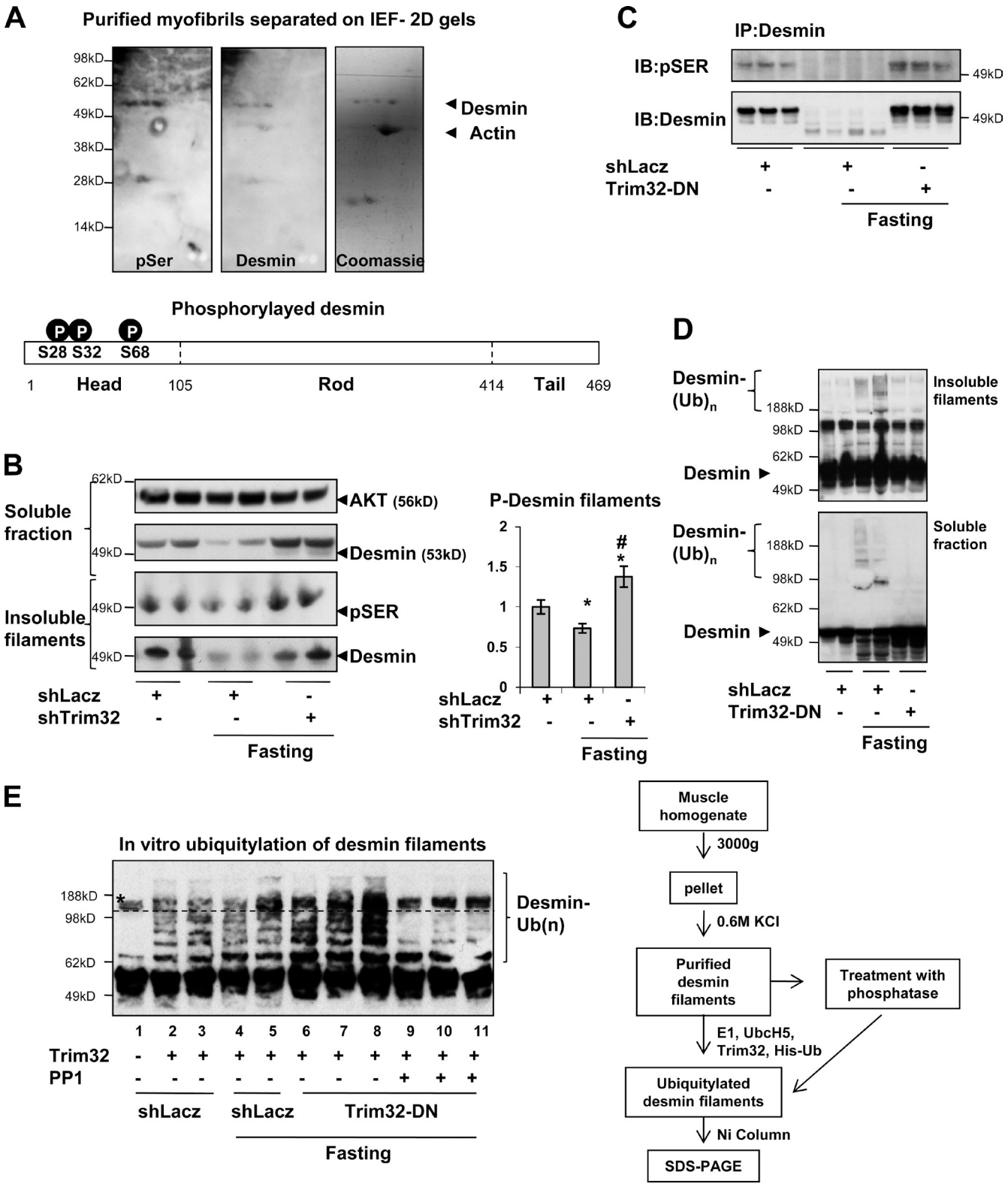

Figure 4. **Trim32 promotes disassembly and destruction of phosphorylated desmin filaments.** (A) Desmin filaments are phosphorylated during fasting. Top: the pellet from atrophying muscle expressing shTrim32 was analyzed by isoelectric focusing 2D gel electrophoresis and Coomassie blue staining. Four spots were observed at ~53 kD and were identified by mass spectrometry as vimentin and desmin phosphorylated at serines 28, 32, and 68. Bottom: the three phosphorylated serine residues are located in desmin's head domain. (B) Trim32 promotes disassembly and destruction of phosphorylated desmin filaments during fasting. Left: desmin filaments were isolated from normal and atrophying muscles expressing shLacz or shTrim32, and analyzed in parallel to the soluble fraction by SDS-PAGE and immunoblotting. Phosphorylated desmin was detected with phospho-serine antibody. The AKT blot serves as a loading control. Right: densitometric measurement of blots which were stained for phospho-serine. *, $P < 0.05$ shTrim32 vs. fed control; #, $P < 0.005$ shTrim32 vs. shLacz in fasting; $n = 13$. (C) During fasting, desmin accumulates as a phosphorylated species in the cytosol of muscles deficient in active Trim32. Desmin was immunoprecipitated from the soluble fraction of muscles expressing shLacz or dominant-negative to Trim32 (Trim32-DN) from

filaments (Fig. 4 B) and of soluble desmin (Fig. 4, B and C) in these shTrim32-expressing muscles exceeded the amounts observed in muscles of fed mice ($P < 0.05$), even though only about half the fibers were transfected. Thus, the phosphorylation of desmin filaments appears to increase during fasting, and Trim32 catalyzes the solubilization and degradation of these phosphorylated proteins.

Furthermore, desmin immunoprecipitation from the soluble fraction of the muscles from fasted mice and immunoblotting with anti–phospho-serine also indicated that during fasting, desmin was released from the cytoskeleton into the cytosol as the phosphorylated species. However, it was then degraded, but not when endogenous Trim32 was inhibited by overexpression of the dominant negative (Fig. 4 C). Interestingly, the antibody used for immunoprecipitation also bound fragments of desmin in the soluble fraction of the atrophying muscle, where Trim32 was functional, but not when this enzyme was inhibited by transfection of the Trim32-DN (Fig. 4 C). Because the appearance of these fragments was dependent on Trim32, they probably were formed by the incomplete degradation of desmin by the proteasome. Thus, Trim32 is essential during fasting for solubilization and destruction of phosphorylated desmin filaments, which may also promote the breakdown of the desmin-associated Z-bands and the attached thin filaments.

Phosphorylation of desmin during fasting increases susceptibility to ubiquitylation by Trim32

These findings suggest that the enhanced phosphorylation of desmin filaments during fasting increases their ubiquitylation by Trim32 and degradation. To determine if Trim32 can ubiquitylate desmin filaments, we isolated desmin filaments from TA muscles of normal and fasted mice that were electroporated with either the Trim32-DN or shLacz. We then analyzed these filaments and the soluble fractions of these muscles by SDS-PAGE and immunoblotting with a desmin antibody. Upon fasting, high molecular weight ubiquitylated species of desmin accumulated as both insoluble filaments and in the soluble fraction (Fig. 4 D). The ubiquitylation of desmin is dependent on Trim32 because these high molecular weight conjugates were not evident in muscles expressing the Trim32-DN (Fig. 4 D). Thus, during fasting, desmin is ubiquitylated and targeted for degradation by Trim32.

To analyze the influence of desmin phosphorylation on its ubiquitylation, we assayed the susceptibility of the purified desmin filaments to ubiquitylation by Trim32 and UbcH5 using 6His-tagged ubiquitin. The 6His-tagged ubiquitylated proteins were isolated and analyzed by SDS-PAGE and immunoblot using an antibody against desmin (Fig. 4 E). Trim32 catalyzed the formation of long ubiquitin chains on desmin filaments isolated from normal muscle (Fig. 4 E, lanes 2 and 3). The filaments purified from the atrophying muscles, in which Trim32 was active and catalyzing desmin degradation, contained fewer phosphorylated proteins (Fig. 4 B), and seemed to be ubiquitylated less by purified Trim32 in vitro (Fig. 4 E, lanes 4 and 5). By contrast, the desmin filaments from the atrophying muscles lacking functional Trim32, whose phosphorylation levels exceeded those in fed control (Fig. 4 B), were even more extensively ubiquitylated by Trim32 than the filaments purified from both fed (Fig. 4 E, compare lanes 6–8 and 2–3) and fasted mice (Fig. 4 E, compare lanes 6–8 and 4–5). In other words, the muscles where Trim32 functioned in vivo contained less phosphorylated desmin, and were modified less by purified Trim32. However, in atrophying muscles lacking Trim32 phosphorylated desmin accumulated and was particularly sensitive to the purified enzyme.

To test more directly if the desmin phosphorylation promotes its ubiquitylation, we treated the desmin fraction from atrophying muscles expressing shTrim32 with the general protein phosphatase 1, PP1. After pretreatment with PP1 (Fig. 4 E, lanes 9–11) these filaments were resistant to ubiquitylation by Trim32, indicating that phosphorylation of desmin filaments enhances their recognition and ubiquitylation by this E3. Thus, during fasting, phosphorylation of desmin filaments increases and facilitates their ubiquitylation by Trim32, depolymerization, and degradation.

Depolymerization of desmin filaments promotes the loss of thin filaments

As shown above, down-regulation of Trim32 during fasting inhibits the loss of thin filaments (Fig. 1 D) and desmin (Fig. 4). Because the integrity of desmin filaments is important for myofibril stability (Huang et al., 2002; Conover et al., 2009), we determined whether this Trim32-dependent degradation of desmin during fasting may help trigger the disassembly and destruction of thin filament proteins. For this purpose, we used a vector encoding the N-terminal region of desmin (Desmin-DN), which functions as a dominant-negative inhibitor of desmin filament assembly (Chen et al., 2003). If these filaments are continuously being formed and depolymerized, then the expression of the truncated mutant should inhibit desmin polymerization and favor its disassembly. We co-electroporated TA muscles with the Trim32-DN and the desmin-DN (to promote dissociation of desmin filaments) and induced atrophy by food deprivation. Depolymerization of desmin filaments was enhanced in these muscles, as shown by the lower amounts of phosphorylated desmin filaments and the resulting greater amounts of soluble desmin than in the atrophying muscles not expressing desmin-DN

fed or fasted mice. Precipitates were analyzed by immunoblotting using anti-desmin and phospho-serine. (D) Trim32 ubiquitylates desmin during fasting in vivo. Desmin filaments, which were purified from normal or atrophying muscles expressing shLacz or Trim32-DN, were analyzed in parallel to the soluble fraction by Western blot analysis using a desmin antibody. (E) Phosphorylation of desmin filaments facilitates their ubiquitylation by Trim32. Isolated desmin filaments from normal (lanes 2 and 3) and atrophying muscles expressing shLacz (lanes 4 and 5) or Trim32-DN (lanes 6–11) were treated with protein phosphatase 1 (PP1; lanes 9–11) or left untreated (lanes 6–8) and then subjected to ubiquitylation by pure Trim32 and UbcH5 using 6His-tagged ubiquitin. The 6His-tagged ubiquitin conjugates were purified with a Ni column and analyzed by SDS-PAGE and immunoblotting using anti-desmin. The band above the dashed line, which is also marked with an asterisk, is nonspecific.

(i.e., coexpressing Trim32-DN and shLacz; Fig. 5 A). The ability of Trim32-DN to protect against loss of muscle mass was not affected by the coexpression of desmin-DN (Fig. 5 B).

To learn whether the enhanced disassembly of desmin filaments accelerates the loss of myofibrillar proteins during fasting, we measured the content of thin and thick filament components in myofibrils (as in Fig. 1 D) purified from muscles, which were co-electroporated with Trim32-DN and either desmin-DN or shLacz. By 2 d of fasting, the total content of myofibrillar proteins decreased by more than 40% in muscles expressing shLacz (Fig. 1 D), but inhibition of Trim32 by expression of Trim32-DN markedly reduced the loss of actin as well as other thin filament and Z-band components. In fact, the content of these proteins did not differ from those in muscles of fed mice (Fig. 5 C). However, MyHC content still decreased significantly in these muscles (Fig. 5 C) as expected because thick filament proteins are degraded primarily by MuRF1 (Cohen et al., 2009).

Interestingly, in the atrophying muscles expressing Trim32-DN, transfection of desmin-DN to cause disassembly of desmin filaments induced a loss of actin, α-actinin, and Tm from the myofibril (Fig. 5 C; $P < 0.05$). In addition, TnI and TnT seemed to show a similar reduction, but these trends did not reach statistical significance. Thus, desmin disassembly can promote breakdown of thin filaments and Z-bands. Surprisingly, the content of MyHC decreased, which suggests that destruction of desmin and thin filaments may also reduce the stability of thick filaments (see Discussion). Thus, the Trim32-dependent breakdown of phosphorylated desmin filaments during fasting enhances destruction of thin filaments by this enzyme, and perhaps other ubiquitin ligases (Lokireddy et al., 2011).

It is also noteworthy that in muscles of fed mice, enhancing depolymerization of desmin filaments by transfection of the desmin-DN did not promote the loss of myofibrillar proteins (Fig. 5 D). Thus, the loss of these proteins during fasting appears to require an additional signal beyond desmin disassembly, presumably the fasting-induced phosphorylation of desmin and perhaps other proteins.

To test further if the loss of desmin precedes and thus may promote degradation of thin filaments and Z-bands, we determined the time course of loss of desmin, actin, and α-actinin during fasting. Immunoblotting of equal amounts of myofibrils from TA muscles of fed mice and ones that were deprived of food for 1 or 2 d showed that the total amounts of actin and α-actinin, as well as MyHC and MyLC, were markedly reduced 2 d after food deprivation. The loss of desmin, however, was already evident 1 d after food deprivation and thus precedes degradation of thin filaments and Z-bands (Fig. 5 E).

Discussion

Trim32 is critical for the loss of thin filaments during fasting

The accelerated degradation of myofibrils is a major contributor to the loss of muscle mass and strength during atrophy. As shown here, during the rapid atrophy induced by fasting, the loss of myofibrillar proteins exceeds the decrease in total muscle mass and soluble proteins. We previously showed that during denervation atrophy, MuRF1 is responsible for the loss of thick filament components (Cohen et al., 2009), and the present studies demonstrate that Trim32 is critical in the rapid degradation of thin filaments and Z-bands upon fasting. Because the loss of contractile proteins is a general feature of muscle wasting, similar mechanisms probably function in other types of muscle wasting. The systemic atrophy of muscle upon fasting is signaled by the low levels of insulin and IGF-1 and increased levels of glucocorticoids, which cause accelerated proteolysis and FoxO-mediated expression of the atrogene program (Sandri et al., 2004), as also occur in most types of rapid muscle wasting. In fasting-induced atrophy, Trim32 plays a critical role, even though its expression does not rise (Fig. 1 E), in contrast to the other atrophy-related E3s, Atrogin1/MAFBx (Gomes et al., 2001) and MuRF1. Interestingly, during atrophy induced by unloading, Trim32 is induced (Kudryashova et al., 2005).

Reducing Trim32 function either by shRNA or a dominant-negative inhibitor markedly attenuated the decrease in fiber diameter and the loss of actin, Tm, and troponins upon fasting. Early studies demonstrated that in muscle extracts, myofibrillar proteins are much more resistant to degradation by the ubiquitin–proteasome system than free actin or myosin (Solomon and Goldberg, 1996). This observation led to the suggestion that myofibrillar proteins must be initially cleaved by calpains (Tidball and Spencer, 2002) or by caspase 3 (Du et al., 2004) before degradation by the ubiquitin–proteasome pathway. However, these conclusions seem unlikely because in mice lacking caspase 3, actin degradation proceeds normally after denervation (Plant et al., 2009). Also, we found that MuRF1 can ubiquitylate myosin and associated regulatory proteins (Cohen et al., 2009), and Trim32 can polyubiquitylate actin while they are in the intact myofibrils (Fig. 2 A). In addition to causing the marked sparing of thin filament proteins, Trim32 down-regulation caused a slight reduction in the loss of myosin upon fasting. Although this marked loss of myosin occurs presumably through MuRF1-dependent ubiquitylation (Fig. 1 D; Cohen et al., 2009), Trim32 may assist MuRF1 in the complete breakdown of thick filament components; for example, in the myofibril, myosin may become accessible to Trim32 after partial dissociation of thick filaments by MuRF1. One thick filament component, MyLC2, can be ubiquitylated by Trim32. However, Trim32 by itself cannot catalyze the loss of thick filaments because they were protected completely from degradation in muscles lacking functional MuRF1 (Cohen et al., 2009).

Trim32 ubiquitylated pure actin more efficiently than MyLC2 (Fig. 2 A) and did not modify MyHC (not depicted). Furthermore, in the intact myofibril, only actin is ubiquitylated by this E3. Thus, Trim32 shows a strong preference for thin filament components and desmin. Because thick filament components, aside from MyLC2, were not ubiquitylated by Trim32, their limited sparing by Trim32 down-regulation (Fig. 1 D) is likely to be an indirect effect. For example, Trim32-dependent destruction of desmin, Z-bands, and thin filaments may lead to structural changes in the thick filaments so as to enhance their sensitivity to ubiquitylation perhaps in the A-band, where actin

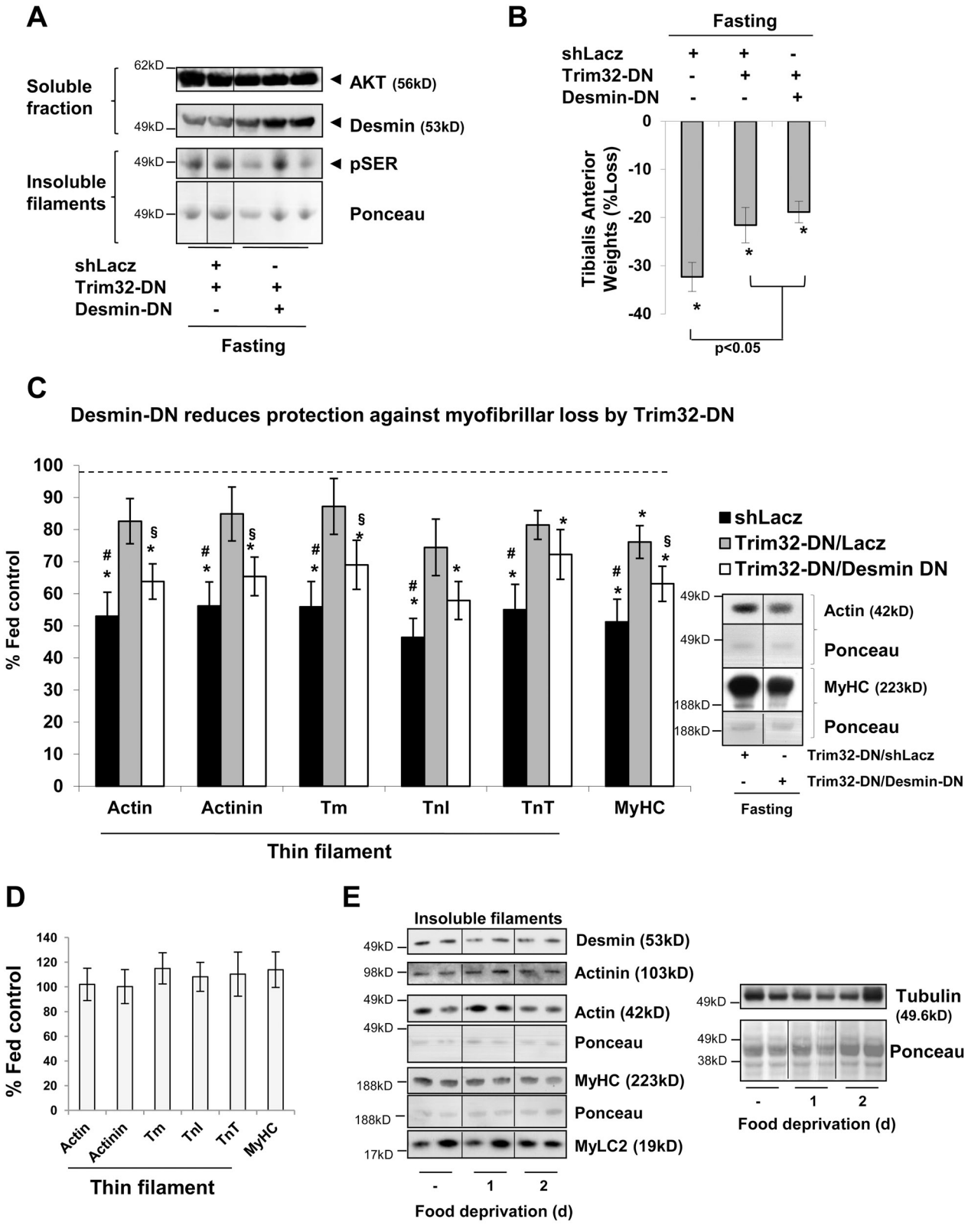

Figure 5. **Depolymerization of desmin filaments promotes the loss of thin filaments during fasting.** To test if disassembly of desmin filaments influences the stability of thin filaments, TA muscles were co-electroporated with Trim32-DN and either shLacz or a dominant-negative mutant of desmin (Desmin-DN) to induce filament disassembly. 4 d later, animals were deprived of food for 2 d. (A) Desmin-DN enhances disassembly of desmin filaments during fasting in muscles expressing Trim32-DN. Isolated desmin filaments and the soluble fraction from transfected muscles were analyzed by SDS-PAGE and immunoblotting. Representative bands were chosen based on similar atrophy rates in transfected muscles. Ponceau S staining is shown as a loading control for the pSER membrane. (B) The ability of Trim32-DN to protect against loss of muscle mass is not affected by the coexpression of desmin-DN. Mean weights of electroporated muscles are plotted as percent weight loss. $n = 6$. *, $P < 0.005$. (C) Depolymerization of desmin filaments by Desmin-DN during fasting

and myosin interact. Also, this small sparing of thick filaments may involve other indirect mechanisms because Trim32 has additional proteins as substrates (e.g., desmin).

In addition to their presence in myofibrils, some actin, Tm, troponins, and myosin were recovered in the soluble fraction. Because these soluble forms were increased after knockdown of Trim32, they seemed to be degraded by a Trim32-dependent mechanism during atrophy. Soluble pools of contractile proteins may represent either newly synthesized precursors of myofibrils or proteins released during myofibrillar turnover, and destined for destruction by proteasomes (Cohen et al., 2009; Neti et al., 2009). Our findings strongly suggest that in atrophying muscles these soluble proteins are primarily intermediates in myofibrillar destruction. Because ubiquitylation of Tm, α-actinin, and MyLC2 by pure Trim32 with UbcH5 was limited, their loss from the soluble fraction of muscle in vivo may require an additional cofactor to function with Trim32 (e.g., a different E2 or an E4). Alternatively, these components in vivo may be modified (e.g., by phosphorylation) before their recognition and ubiquitylation by Trim32, as we found for desmin.

It is also noteworthy that down-regulation of Trim32 led to a dramatic decrease in fiber and muscle atrophy that cannot be explained solely by stabilization of thin filaments. Actin comprises only 25% of the weight of myofibrils, and myosin, the major myofibrillar constituent, is still degraded in the absence of Trim32. In addition, many soluble proteins and organelles are digested by autophagy (Mammucari et al., 2007; Zhao et al., 2007). Thus, there must be important nonmyofibrillar substrates for Trim32, which accumulate when this enzyme is down-regulated and have a large, perhaps regulatory effect, to increase fiber size.

Trim32 preferentially modifies phosphorylated desmin

Our initial microarray studies identified a set of "atrogenes" (atrophy-related genes), which are induced or repressed similarly in diverse wasting conditions (Lecker et al., 2004; Sacheck et al., 2007), but an additional group of genes (>200) was found to be induced specifically upon disuse or denervation (Sacheck et al., 2007). Because Trim32 is up-regulated upon unloading (Kudryashova et al., 2005) but not during fasting, it might be induced specifically in the slower atrophy resulting from inactivity. Therefore, we hypothesized that during fasting there are post-translational modifications of Trim32's substrates that enhance their ubiquitylation. Accordingly, down-regulation of Trim32 in mouse muscle during fasting resulted in an accumulation of phosphorylated desmin filaments to levels that exceeded those in muscles from fed mice. Thus, the phosphorylation of desmin filaments must increase during fasting, leading to enhanced ubiquitylation by Trim32, disassembly, and degradation.

The strongest evidence for the importance of desmin phosphorylation was our finding that phosphatase treatment markedly reduced its ubiquitylation by Trim32. It is unusual for a ring finger ubiquitin ligase such as Trim32 to act preferentially on phosphorylated substrates (which is usually a property of SCF E3s), although C-Cbl is known to ubiquitylate phosphorylated tyrosine kinase receptors (Joazeiro et al., 1999). Perhaps phosphorylation of Trim32's other substrates also enhances their recognition by this enzyme, although phosphorylation cannot be a prerequisite for ubiquitylation by Trim32 because this enzyme modifies pure actin and Tm in vitro (Fig. 2 A).

During fasting, phosphorylation of desmin occurred on serine 28, 32, and 68 within desmin's head domain. Phosphorylation of serines in this domain was reported to promote disassembly of desmin filaments (Inagaki et al., 1987). The rod domains of neighboring desmin molecules interact to create the IF backbone, but the head domains must be accessible for phosphorylation and binding of factors that promote cytoskeletal reorganization (Geisler and Weber, 1988), such as Trim32. Several kinases, including PKA, PKC, Ca^{2+}/calmodulin kinase II, cdc2 kinase, and Rho-kinase, can phosphorylate desmin filaments within the head domain and affect filament structure (Inagaki et al., 1996; Kawajiri et al., 2003). It is unclear if any of these kinases is activated in muscle during fasting and phosphorylates desmin. One good candidate is PKC because desmin phosphorylation by this kinase is related to the disarray of the myofibrils in cardiomyocytes (Huang et al., 2002), and activation of PKC in muscle induces proteolysis (Wyke and Tisdale, 2006). Together, these findings argue strongly that the increased phosphorylation of desmin filaments during fasting enhances their ubiquitylation by Trim32, leading to filament disassembly and degradation (Fig. 6). The solubilization of the ubiquitylated desmin and the subsequent release of myofibrillar components may also involve the p97–VCP ATPase complex (Rabinovich et al., 2002), which extracts ubiquitylated proteins from larger structures (e.g., the ER membrane in the ERAD pathway) before proteasomal degradation.

Disassembly of desmin filaments is linked to the destruction of thin filaments during fasting

These studies demonstrate that cytoskeletal modifications occur during fasting and appear to promote myofibrillar breakdown.

reduces the sparing of thin filament proteins and MyHC by Trim32-DN. Left: myofibrils purified from atrophying muscles expressing shLacz alone (black bars), Trim32-DN together with shLacz (shaded bars), or Trim32-DN together with Desmin-DN (open bars) were analyzed by SDS-PAGE and Coomassie blue staining. The absolute content of each myofibrillar protein was obtained as described in Fig. 1 D. Data are expressed as percentages of fed control. $n = 10$, *, $P < 0.05$ vs. fed control; #, $P < 0.05$ vs. Trim32-DN/Lacz; §, $P < 0.05$ vs. Trim32-DN/Lacz. Right: equal fractions of myofibrils from different muscle samples were analyzed by immunoblotting using anti-actin and anti-MyHC. Ponceau S staining is shown as a loading control for each membrane. (D) Electroporation of desmin-DN into normal muscle to promote desmin disassembly does not trigger destruction of thin filaments. Myofibrils from normal muscles expressing desmin-DN were analyzed by SDS-PAGE and Coomassie blue staining, and the absolute content of each protein was calculated as in Fig. 1 D. Data are presented as percentage of control (expressing shLacz). $n = 6$. (E) During fasting, loss of desmin precedes degradation of myofibrillar proteins and Z-bands. Time course of the loss of desmin and myofibrillar proteins was analyzed by immunoblotting of equal amounts of myofibrils from TA muscles of fed mice and ones deprived of food for 1 or 2 d. Representative bands were chosen based on similar atrophy rates. Ponceau S staining is shown as a loading control.

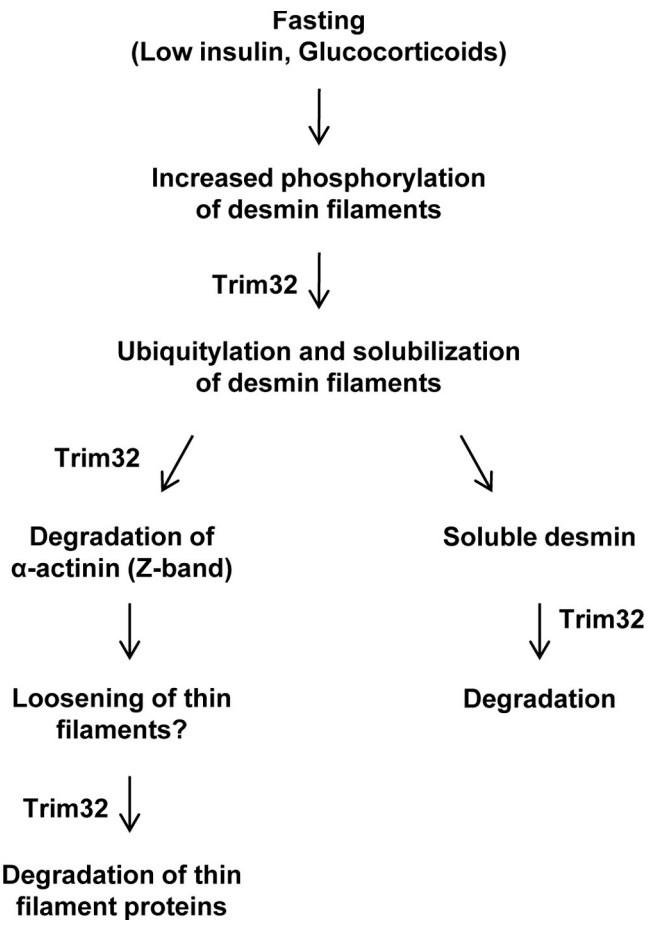

Figure 6. **Proposed mechanism for thin filament loss during atrophy.** Upon fasting, when insulin and IGF-1 levels are low and glucocorticoid levels rise, there is an enhanced phosphorylation of desmin filaments leading to ubiquitylation by Trim32 (Fig. 4), disassembly, and degradation (Fig. 3). Because desmin filaments are important for the stability of the Z-band (Fuseler and Shay, 1982) and the attached thin filaments (Conover et al., 2009), this loss of desmin filaments probably loosens the structure of the Z-band and reduces the stability of thin filaments (Fig. 6). As a result, Z-band components (e.g., α-actinin) as well as actin and associated thin filament proteins should be more susceptible to ubiquitylation by Trim32.

In muscles deficient in Trim32, the loss of thin filaments and desmin filaments were both decreased upon fasting. Furthermore, transfection of a truncated desmin mutant that promotes disassembly of desmin filaments enhanced the destruction of thin filaments during fasting, even in muscles deficient in Trim32. Therefore, this destructive process may also be catalyzed by another E3 in the absence of Trim32 (Lokireddy et al., 2011), provided there is an alternative mechanism causing disassembly of desmin filaments. However, Trim32 must be the important ubiquitin ligase causing thin filaments loss during fasting because its down-regulation prevents thin filament breakdown, and it catalyzes ubiquitylation of multiple thin filament proteins, especially actin, as well as desmin and α-actinin.

During myogenesis, desmin associates with the developing myofibrils and aligns them at the Z-lines across the sarcomere (Fuseler and Shay, 1982). Because actin filaments are anchored at the Z-lines, their structural integrity is likely to be compromised by the loss of the Z-band component, α-actinin, which results from depolymerization and destruction of desmin filaments. In fact, in cardiomyocytes, expression of a mutant desmin that displaces endogenous desmin from the Z-lines markedly perturbs thin filament architecture (Conover et al., 2009). Furthermore, desmin missense mutations cause a cardiomyopathy characterized by myofibrillar disarray leading to heart failure (Otten et al., 2010). Because intact desmin filaments are important for Z-band and thin filament stability, the loss of desmin filaments during fasting probably loosens the highly ordered structure of Z-lines and compromises the structural integrity of thin filaments (Fig. 6). As a result, Z-band components as well as actin and associated proteins should now be more accessible and susceptible to ubiquitylation by Trim32 (Fig. 6).

An autosomal-recessive mutation in Trim32's third NHL repeat (D487N) is one of the causes for limb girdle muscular dystrophy 2H (LGMD-2H; Frosk et al., 2002). If this mutation causes a gain or loss of enzymatic function, then it might perturb myofibrillar organization and stability. However, the biochemical alterations in these muscles are still unclear, and the effects of this mutation on Trim32 activity are debated (Kudryashova et al., 2005; Locke et al., 2009) and require in-depth study based upon the present identification of its substrates and physiological roles. Moreover, it remains uncertain if Trim32 also functions in the slower turnover of thin filament proteins in normal muscle.

Because Trim32 is ubiquitously expressed, it is likely to have important roles in other tissues, not only in cardiac and smooth muscle, but also in epithelia and brain, where its level is especially high (Kudryashova et al., 2009). In addition to LGMD-2H, Trim32 mutations can cause Bardet-Biedl syndrome (Chiang et al., 2006), which is characterized by retinal degeneration, obesity, cognitive impairment, and renal and cardiovascular anomalies. Up-regulation of Trim32 has been reported in several types of cancer (Horn et al., 2004; Kano et al., 2008), in the occipital lobe of patients with Alzheimer's disease (Yokota et al., 2006), and in psoriasis lesions (Liu et al., 2010). Because Trim32 is a critical regulator of cytoskeletal and actin levels during muscle atrophy, in other cells it may also influence cell polarity, cell division, mobility, metastasis, and neuronal function, all of which are dependent upon alterations in the cytoskeleton and actin filament architecture.

Materials and methods

In vivo transfection

All animal experiments were consistent with the National Institutes of Health Guide for the Care and Use of Laboratory Animals and conducted according to the ethical guidelines. Animal care was provided by specialized personnel in the Institutional Animal Care facility. In vivo electroporation experiments were performed in adult CD-1 male mice (27–28 g) as described previously (Brault et al., 2010). In brief, 20 µg of plasmid DNA was injected into adult mouse TA muscles, and electric pulses applied by two electrodes, which were place underneath and on top of the muscle (12 V, 5 pulses, 200-ms intervals). In fasting experiments food was removed from cages 4 d after electroporation.

Excised muscles were snap-frozen in isopentane and cross sections were fixed in 4% PFA. Cross-sectional area of transfected (express GFP) and adjacent nontransfected fibers in the same muscle section (10 µm) was measured using MetaMorph (Molecular Devices), and data collected from at least 450 fibers from 6 mice were plotted on a graph. Individual fiber size was determined in the entire muscle cross section by laminin staining

(using a 1:50 dilution of laminin antibody and a 1:1,000 dilution of Alexa Fluor 555–conjugated secondary antibody). Images were collected using an upright epifluorescence microscope (model 80i; Nikon) with a Plan Fluor 40x 1.4 NA or Plan Apo 20x 0.75 NA objective lens, a 545/30 excitation filter and 620/60 emission filter (Chroma Technology Corp.), a cooled CCD camera (model C8484-03; Hamamatsu Photonics), and MetaMorph software.

Plasmid DNA and generation of shRNA

The shRNA oligos against Trim32 (Table S2) and Lacz were designed using Invitrogen's RNAi designer tool and were cloned into pcDNA 6.2-GW/EmGFP-miR vector using Invitrogen's BLOCK-iT RNAi expression vector kit. The pCGN-HA construct encoding the dominant-negative Trim32 mutant contains human Trim32 cDNA lacking the RING domain (aa 1–65), and has been described previously (Kano et al., 2008). The mammalian expression vector encoding the N-terminal region of desmin was obtained from Vincent Cryns (Northwestern University, Evanston, IL).

Antibodies and materials

Anti-actin, actinin, phospho-serine, laminin, and GAPDH were purchased from Sigma-Aldrich. Anti-MyHC, tropomyosin, and desmin were from Abcam; anti-tubulin from Invitrogen; and anti-AKT from Cell Signaling Technology. Anti-MyLC2 (developed by Donald A. Fischman) was obtained from Developmental Studies Hybridoma Bank (University of Iowa, Iowa City, IA) under the auspices of the National Institute of Child Health and Human Development. The MyBP-C antibody was kindly provided by Marion Greaser (University of Wisconsin-Madison, Madison, WI), and the Trim32 antibody by Juergen Knoblich (Institute of Molecular Biotechnology, Vienna, Austria). UbcH13/Uev1 E2-conjugating enzyme was purchased from Boston Biochem, and UbcH5 clone was provided by Kazuhiro Iwai (Osaka City University, Osaka, Japan).

Fractionation of muscle tissue

Muscles were homogenized in cold buffer (20 mM Tris-HCl, pH 7.2, 5 mM EGTA, 100 mM KCl, and 1% Triton X-100) and myofibrils isolated by centrifugation at 3,000 *g* for 30 min at 4°C (Cohen et al., 2009). The myofibrillar pellet was washed two times in wash buffer (20 mM Tris-HCl, pH 7.2, 100 mM KCl, and 1 mM DTT), and after final centrifugation (3,000 *g* for 10 min at 4°C) was resuspended in storage buffer (20 mM Tris-HCl, pH 7.2, 100 mM KCl, 1 mM DTT, and 20% glycerol) and kept at −80°C.

To purify desmin filaments from extracted myofibrils, myofibrillar pellets (equivalent to 0.1% of muscle weight) were resuspended in ice-cold extraction buffer (0.6 M KCl, 1% Triton X-100, 2 mM EDTA, 1 mM DTT, 2 mM PMSF, 10 µg/ml leupeptin, 3 mM benzamidine, 1 µg/ml trypsin inhibitor, and 1x PBS) for 10 min (truncated forms of phosphorylated desmin may appear) with shaking at 4°C, spun at 3,000 *g* for 10 min at 4°C, and then washed briefly with extraction buffer.

Protein analysis

All assays were performed as described previously (Cohen et al., 2009). To determine the absolute content of each myofibrillar protein, equal amounts of isolated myofibrils from transfected muscles were analyzed by SDS-PAGE and Coomassie blue staining, and the intensity of specific bands was measured by densitometry. The density of each band was multiplied by the total amount of myofibrillar proteins per muscle and then by the total muscle weight: (band intensity [AU] per mg myofibrils) x (total myofibrils [mg] per muscle) x (muscle weight [mg]). Data in atrophying muscles were presented as percentage of fed control.

For immunoblotting, soluble or myofibrillar fractions from TA muscles as well as the in vitro ubiquitylation reactions were resolved by SDS-PAGE, transferred onto PVDF membranes, and immunoblotted with specific antibodies and secondary antibodies conjugated to alkaline phosphatase. Immunoprecipitation of desmin from the soluble fraction of muscle (Fig. 4 C) was performed overnight at 4°C and then protein A/G–agarose was added for 4 h. Phosphatase inhibitors were not added to lysis buffer except for the immunoprecipitation experiment, in which 1 mM Na_3VO_4 and 50 mM NaF were added. Isoelectric Focusing 2D gel electrophoresis was performed with a pH gradient of 3–10 on a 4–12% gradient gel.

Desmin filaments, which were purified as described above (see Fractionation of muscle tissue), were treated or left untreated with 25 U of protein phosphatase 1 (P0754S; BioLabs) for 1 h at 30°C, and then were washed three times with ubiquitylation reaction buffer (2 mM ATP, 20 mM Tris-HCl, pH 7.6, 20 mM KCl, 5 mM $MgCl_2$, and 1 mM DTT). Trim32's ability to ubiquitylate the washed filaments was then assayed for 90 min at 37°C in 20-µl mixtures containing 22.5 nM E1, 0.75 µM UbcH5, 0.4 µM Trim32, and 59 µM His-ubiquitin in ubiquitylation reaction buffer. The His-tagged ubiquitin conjugates were purified with Ni-beads (according to the manufacturer's instructions) and analyzed by SDS-PAGE and immunoblotting with anti-desmin.

For mass spectrometry, purified samples were digested with trypsin and analyzed by nanoscale-microcapillary reversed-phase liquid chromatography tandem mass spectrometry (LC-MS/MS). Peptides were separated across a 45-min gradient ranging from 5 to 35% (vol/vol) acetonitrile in 0.1% (vol/vol) formic acid in a microcapillary (125 µm x 18 cm) column packed with C18 reverse-phase material (Magic C18AQ, 5-µm particles, 200 Å pore size; Michrom Bioresources) and on-line analyzed on the LTQ Orbitrap XL or LTQ Orbitrap Discovery hybrid FTMS (Thermo Fisher Scientific). For each cycle, one full MS scan acquired on the Orbitrap at high mass resolution was followed by ten MS/MS spectra on the linear ion trap from the ten most abundant ions. MS/MS spectra were searched using the SEQUEST algorithm against a concatenated forward/reverse mouse IPI (ver 3.60) database with dynamic modification of methionine oxidation. All peptide matches were filtered based on mass deviation, charge, XCorr, and dCn to a target peptide false discovery rate (FDR) of 1% using linear discriminant analysis (LDA) to distinguish between forward and reverse hits.

Immunofluorescence labeling of paraffin-embedded muscle sections

Paraffin-embedded longitudinal sections of TA from fed and fasted mice were cut at 10 µm. To remove paraffin, slides were immersed in xylene for 5 min, and then were gradually rehydrated in 100, 95, 50, 25, 0% ethanol/PBS. Immunofluorescence analysis on the rehydrated sections was performed using a 1:50 dilution of desmin antibody and a 1:1,000 dilution of Alexa Fluor 555–conjugated secondary antibody, both diluted in blocking solution (50 mg/ml BSA/TBS-T). Images were collected at room temperature using an upright epifluorescence microscope (model 80i; Nikon) with a Plan Fluor 40x 1.4 NA objective lens, a 545/30 excitation filter and 620/60 emission filter (Chroma Technology Corp.), a cooled CCD camera (model C8484-03; Hamamatsu Photonics), and MetaMorph software.

Quantitative real-time PCR

Total RNA was isolated from muscle using TRIzol reagent (15596–018; Invitrogen) and served as a template for synthesis of cDNA by reverse transcription. Real-time qPCR was performed on mouse target genes using specific primers (Table S2) and DyNAmo HS SYBR Green qPCR kit (F-410S; Finnzymes) according to the manufacturer's protocol.

Statistical analysis and image acquisition

Data are presented as means ± SEM. The statistical significance was accessed with the paired Student's *t* test. Muscle sections were imaged at room temperature with an upright fluorescent microscope (model 80i; Nikon) and a monochrome camera (C8484-03; Hamamatsu Photonics). Image acquisition and processing was performed using MetaMorph software. Black and white images were processed with Adobe Photoshop CS3, version 10.0.1 software.

Online supplemental material

Fig. S1 shows that down-regulation of Trim32 does not affect fiber size 4 d after electroporation. In addition, it includes representative cross sections of muscles from fasted mice expressing shTrim32, and representative Coomassie blue–stained gels used for densitometric measurements of specific myofibrillar components. Fig. S2 shows that after incubation of muscle pellet with 0.6 M KCl myofibrils almost fully disassemble, whereas desmin filaments are stable. Table S1 includes the raw data that were used for the calculation of the total amounts of each myofibrillar protein per muscle, and the percent sparing of each protein in atrophying muscles expressing shTrim32. Table S2 contains a list of qPCR primers and shRNA oligos that were used in the present study. Online supplemental material is available at http://www.jcb.org/cgi/content/full/jcb.201110067/DC1.

We thank Dr. Olga Kandror for all her assistance and support, and Mary Dethavong for her help in preparing this manuscript. We are grateful to Drs. Donghoon Lee and Jinghui Zhao for their help with the animal work, and the Nikon Imaging Center at Harvard Medical School for their assistance in fluorescence microscopy.

This project was supported by grants from the National Institute of Aging, Muscular Dystrophy Association, and the Packard Foundation to A.L. Goldberg; and a stipend to S. Cohen from the International Sephardic Education Foundation (ISEF).

Submitted: 17 October 2011
Accepted: 13 July 2012

Note added in proof. After this paper was accepted for publication, Kudryashova et al. (2012. *J. Clin. Invest.* doi:10.1172/JCI59581) reported that muscles from Trim32-null mice atrophy similarly to WT upon fasting or disuse. However, these Trim32 knockout mice exhibit myopathies, neurogenic defects, and reduced normal muscle growth (e.g., fast myofibers are smaller than the WT). Because Trim32 is important for normal muscle growth and homeostasis, muscles of mice lacking Trim32 seem inappropriate systems to explore myofibrillar turnover and the mechanisms of atrophy. Here, we addressed such questions using transient electroporation to reduce Trim32 levels in normal adult muscles to avoid possible developmental effects.

References

Bodine, S.C., E. Latres, S. Baumhueter, V.K. Lai, L. Nunez, B.A. Clarke, W.T. Poueymirou, F.J. Panaro, E. Na, K. Dharmarajan, et al. 2001. Identification of ubiquitin ligases required for skeletal muscle atrophy. *Science*. 294:1704–1708. http://dx.doi.org/10.1126/science.1065874

Boudriau, S., C.H. Côté, M. Vincent, P. Houle, R.R. Tremblay, and P.A. Rogers. 1996. Remodeling of the cytoskeletal lattice in denervated skeletal muscle. *Muscle Nerve*. 19:1383–1390. http://dx.doi.org/10.1002/(SICI)1097-4598(199611)19:11<1383::AID-MUS2>3.0.CO;2-8

Brault, J.J., J.G. Jespersen, and A.L. Goldberg. 2010. Peroxisome proliferator-activated receptor gamma coactivator 1alpha or 1beta overexpression inhibits muscle protein degradation, induction of ubiquitin ligases, and disuse atrophy. *J. Biol. Chem.* 285:19460–19471. http://dx.doi.org/10.1074/jbc.M110.113092

Chen, F., R. Chang, M. Trivedi, Y. Capetanaki, and V.L. Cryns. 2003. Caspase proteolysis of desmin produces a dominant-negative inhibitor of intermediate filaments and promotes apoptosis. *J. Biol. Chem.* 278:6848–6853. http://dx.doi.org/10.1074/jbc.M212021200

Chiang, A.P., J.S. Beck, H.J. Yen, M.K. Tayeh, T.E. Scheetz, R.E. Swiderski, D.Y. Nishimura, T.A. Braun, K.Y. Kim, J. Huang, et al. 2006. Homozygosity mapping with SNP arrays identifies TRIM32, an E3 ubiquitin ligase, as a Bardet-Biedl syndrome gene (BBS11). *Proc. Natl. Acad. Sci. USA*. 103:6287–6292. http://dx.doi.org/10.1073/pnas.0600158103

Clarke, B.A., D. Drujan, M.S. Willis, L.O. Murphy, R.A. Corpina, E. Burova, S.V. Rakhilin, T.N. Stitt, C. Patterson, E. Latres, and D.J. Glass. 2007. The E3 Ligase MuRF1 degrades myosin heavy chain protein in dexamethasone-treated skeletal muscle. *Cell Metab.* 6:376–385. http://dx.doi.org/10.1016/j.cmet.2007.09.009

Cohen, S., J.J. Brault, S.P. Gygi, D.J. Glass, D.M. Valenzuela, C. Gartner, E. Latres, and A.L. Goldberg. 2009. During muscle atrophy, thick, but not thin, filament components are degraded by MuRF1-dependent ubiquitylation. *J. Cell Biol.* 185:1083–1095. http://dx.doi.org/10.1083/jcb.200901052

Conover, G.M., S.N. Henderson, and C.C. Gregorio. 2009. A myopathy-linked desmin mutation perturbs striated muscle actin filament architecture. *Mol. Biol. Cell*. 20:834–845. http://dx.doi.org/10.1091/mbc.E08-07-0753

Du, J., X. Wang, C. Miereles, J.L. Bailey, R. Debigare, B. Zheng, S.R. Price, and W.E. Mitch. 2004. Activation of caspase-3 is an initial step triggering accelerated muscle proteolysis in catabolic conditions. *J. Clin. Invest.* 113:115–123.

Fielitz, J., M.S. Kim, J.M. Shelton, S. Latif, J.A. Spencer, D.J. Glass, J.A. Richardson, R. Bassel-Duby, and E.N. Olson. 2007. Myosin accumulation and striated muscle myopathy result from the loss of muscle RING finger 1 and 3. *J. Clin. Invest.* 117:2486–2495. http://dx.doi.org/10.1172/JCI32827

Frosk, P., T. Weiler, E. Nylen, T. Sudha, C.R. Greenberg, K. Morgan, T.M. Fujiwara, and K. Wrogemann. 2002. Limb-girdle muscular dystrophy type 2H associated with mutation in TRIM32, a putative E3-ubiquitin-ligase gene. *Am. J. Hum. Genet.* 70:663–672. http://dx.doi.org/10.1086/339083

Fuseler, J.W., and J.W. Shay. 1982. The association of desmin with the developing myofibrils of cultured embryonic rat heart myocytes. *Dev. Biol.* 91:448–457. http://dx.doi.org/10.1016/0012-1606(82)90051-3

Geisler, N., and K. Weber. 1982. The amino acid sequence of chicken muscle desmin provides a common structural model for intermediate filament proteins. *EMBO J.* 1:1649–1656.

Geisler, N., and K. Weber. 1988. Phosphorylation of desmin in vitro inhibits formation of intermediate filaments; identification of three kinase A sites in the aminoterminal head domain. *EMBO J.* 7:15–20.

Gomes, M.D., S.H. Lecker, R.T. Jagoe, A. Navon, and A.L. Goldberg. 2001. Atrogin-1, a muscle-specific F-box protein highly expressed during muscle atrophy. *Proc. Natl. Acad. Sci. USA*. 98:14440–14445. http://dx.doi.org/10.1073/pnas.251541198

Helliwell, T.R., O. Gunhan, and R.H. Edwards. 1989. Lectin binding and desmin expression during necrosis, regeneration, and neurogenic atrophy of human skeletal muscle. *J. Pathol.* 159:43–51. http://dx.doi.org/10.1002/path.1711590111

Horn, E.J., A. Albor, Y. Liu, S. El-Hizawi, G.E. Vanderbeek, M. Babcock, G.T. Bowden, H. Hennings, G. Lozano, W.C. Weinberg, and M. Kulesz-Martin. 2004. RING protein Trim32 associated with skin carcinogenesis has anti-apoptotic and E3-ubiquitin ligase properties. *Carcinogenesis*. 25:157–167. http://dx.doi.org/10.1093/carcin/bgh003

Huang, X., J. Li, D. Foster, S.L. Lemanski, D.K. Dube, C. Zhang, and L.F. Lemanski. 2002. Protein kinase C-mediated desmin phosphorylation is related to myofibril disarray in cardiomyopathic hamster heart. *Exp. Biol. Med. (Maywood)*. 227:1039–1046.

Inagaki, M., Y. Nishi, K. Nishizawa, M. Matsuyama, and C. Sato. 1987. Site-specific phosphorylation induces disassembly of vimentin filaments in vitro. *Nature*. 328:649–652. http://dx.doi.org/10.1038/328649a0

Inagaki, N., K. Tsujimura, J. Tanaka, M. Sekimata, Y. Kamei, and M. Inagaki. 1996. Visualization of protein kinase activities in single cells by antibodies against phosphorylated vimentin and GFAP. *Neurochem. Res.* 21:795–800. http://dx.doi.org/10.1007/BF02532302

Jackman, R.W., and S.C. Kandarian. 2004. The molecular basis of skeletal muscle atrophy. *Am. J. Physiol. Cell Physiol.* 287:C834–C843. http://dx.doi.org/10.1152/ajpcell.00579.2003

Joazeiro, C.A., S.S. Wing, H. Huang, J.D. Leverson, T. Hunter, and Y.C. Liu. 1999. The tyrosine kinase negative regulator c-Cbl as a RING-type, E2-dependent ubiquitin-protein ligase. *Science*. 286:309–312. http://dx.doi.org/10.1126/science.286.5438.309

Kano, S., N. Miyajima, S. Fukuda, and S. Hatakeyama. 2008. Tripartite motif protein 32 facilitates cell growth and migration via degradation of Abl-interactor 2. *Cancer Res.* 68:5572–5580. http://dx.doi.org/10.1158/0008-5472.CAN-07-6231

Kaufmann, E., K. Weber, and N. Geisler. 1985. Intermediate filament forming ability of desmin derivatives lacking either the amino-terminal 67 or the carboxy-terminal 27 residues. *J. Mol. Biol.* 185:733–742. http://dx.doi.org/10.1016/0022-2836(85)90058-0

Kawajiri, A., Y. Yasui, H. Goto, M. Tatsuka, M. Takahashi, K. Nagata, and M. Inagaki. 2003. Functional significance of the specific sites phosphorylated in desmin at cleavage furrow: Aurora-B may phosphorylate and regulate type III intermediate filaments during cytokinesis coordinatedly with Rho-kinase. *Mol. Biol. Cell*. 14:1489–1500. http://dx.doi.org/10.1091/mbc.E02-09-0612

Kudryashova, E., D. Kudryashov, I. Kramerova, and M.J. Spencer. 2005. Trim32 is a ubiquitin ligase mutated in limb girdle muscular dystrophy type 2H that binds to skeletal muscle myosin and ubiquitinates actin. *J. Mol. Biol.* 354:413–424. http://dx.doi.org/10.1016/j.jmb.2005.09.068

Kudryashova, E., J. Wu, L.A. Havton, and M.J. Spencer. 2009. Deficiency of the E3 ubiquitin ligase TRIM32 in mice leads to a myopathy with a neurogenic component. *Hum. Mol. Genet.* 18:1353–1367. http://dx.doi.org/10.1093/hmg/ddp036

Kudryashova, E., A. Struyk, E. Mokhonova, S.C. Cannon, and M.J. Spencer. 2011. The common missense mutation D489N in TRIM32 causing limb girdle muscular dystrophy 2H leads to loss of the mutated protein in knock-in mice resulting in a Trim32-null phenotype. *Hum. Mol. Genet.* 20:3925–3932. http://dx.doi.org/10.1093/hmg/ddr311

Lazarides, E. 1978. The distribution of desmin (100 A) filaments in primary cultures of embryonic chick cardiac cells. *Exp. Cell Res.* 112:265–273. http://dx.doi.org/10.1016/0014-4827(78)90209-4

Lazarides, E., and B.D. Hubbard. 1976. Immunological characterization of the subunit of the 100 A filaments from muscle cells. *Proc. Natl. Acad. Sci. USA*. 73:4344–4348. http://dx.doi.org/10.1073/pnas.73.12.4344

Lecker, S.H., R.T. Jagoe, A. Gilbert, M. Gomes, V. Baracos, J. Bailey, S.R. Price, W.E. Mitch, and A.L. Goldberg. 2004. Multiple types of skeletal muscle atrophy involve a common program of changes in gene expression. *FASEB J.* 18:39–51. http://dx.doi.org/10.1096/fj.03-0610com

Lecker, S.H., A.L. Goldberg, and W.E. Mitch. 2006. Protein degradation by the ubiquitin-proteasome pathway in normal and disease states. *J. Am. Soc. Nephrol.* 17:1807–1819. http://dx.doi.org/10.1681/ASN.2006010083

Li, J.B., and A.L. Goldberg. 1976. Effects of food deprivation on protein synthesis and degradation in rat skeletal muscles. *Am. J. Physiol.* 231:441–448.

Li, Z., M. Mericskay, O. Agbulut, G. Butler-Browne, L. Carlsson, L.E. Thornell, C. Babinet, and D. Paulin. 1997. Desmin is essential for the tensile strength and integrity of myofibrils but not for myogenic commitment, differentiation, and fusion of skeletal muscle. *J. Cell Biol.* 139:129–144. http://dx.doi.org/10.1083/jcb.139.1.129

Liu, Y., J.P. Lagowski, S. Gao, J.H. Raymond, C.R. White, and M.F. Kulesz-Martin. 2010. Regulation of the psoriatic chemokine CCL20 by E3 ligases Trim32 and Piasy in keratinocytes. *J. Invest. Dermatol.* 130:1384–1390. http://dx.doi.org/10.1038/jid.2009.416

Locke, M., C.L. Tinsley, M.A. Benson, and D.J. Blake. 2009. TRIM32 is an E3 ubiquitin ligase for dysbindin. *Hum. Mol. Genet.* 18:2344–2358. http://dx.doi.org/10.1093/hmg/ddp167

Lokireddy, S., C. McFarlane, X. Ge, H. Zhang, S.K. Sze, M. Sharma, and R. Kambadur. 2011. Myostatin induces degradation of sarcomeric proteins through a Smad3 signaling mechanism during skeletal muscle wasting. *Mol. Endocrinol.* 25:1936–1949. http://dx.doi.org/10.1210/me.2011-1124

Mammucari, C., G. Milan, V. Romanello, E. Masiero, R. Rudolf, P. Del Piccolo, S.J. Burden, R. Di Lisi, C. Sandri, J. Zhao, et al. 2007. FoxO3 controls autophagy in skeletal muscle in vivo. *Cell Metab.* 6:458–471. http://dx.doi.org/10.1016/j.cmet.2007.11.001

Milner, D.J., G. Weitzer, D. Tran, A. Bradley, and Y. Capetanaki. 1996. Disruption of muscle architecture and myocardial degeneration in mice lacking desmin. *J. Cell Biol.* 134:1255–1270. http://dx.doi.org/10.1083/jcb.134.5.1255

Neti, G., S.M. Novak, V.F. Thompson, and D.E. Goll. 2009. Properties of easily releasable myofilaments: are they the first step in myofibrillar protein turnover? *Am. J. Physiol. Cell Physiol.* 296:C1383–C1390. http://dx.doi.org/10.1152/ajpcell.00022.2009

Otten, E., A. Asimaki, A. Maass, I.M. van Langen, A. van der Wal, N. de Jonge, M.P. van den Berg, J.E. Saffitz, A.A. Wilde, J.D. Jongbloed, and J.P. van Tintelen. 2010. Desmin mutations as a cause of right ventricular heart failure affect the intercalated disks. *Heart Rhythm.* 7:1058–1064. http://dx.doi.org/10.1016/j.hrthm.2010.04.023

Plant, P.J., J.R. Bain, J.E. Correa, M. Woo, and J. Batt. 2009. Absence of caspase-3 protects against denervation-induced skeletal muscle atrophy. *J. Appl. Physiol.* 107:224–234. http://dx.doi.org/10.1152/japplphysiol.90932.2008

Rabinovich, E., A. Kerem, K.U. Fröhlich, N. Diamant, and S. Bar-Nun. 2002. AAA-ATPase p97/Cdc48p, a cytosolic chaperone required for endoplasmic reticulum-associated protein degradation. *Mol. Cell. Biol.* 22:626–634. http://dx.doi.org/10.1128/MCB.22.2.626-634.2002

Sacheck, J.M., J.P. Hyatt, A. Raffaello, R.T. Jagoe, R.R. Roy, V.R. Edgerton, S.H. Lecker, and A.L. Goldberg. 2007. Rapid disuse and denervation atrophy involve transcriptional changes similar to those of muscle wasting during systemic diseases. *FASEB J.* 21:140–155. http://dx.doi.org/10.1096/fj.06-6604com

Sandri, M., C. Sandri, A. Gilbert, C. Skurk, E. Calabria, A. Picard, K. Walsh, S. Schiaffino, S.H. Lecker, and A.L. Goldberg. 2004. Foxo transcription factors induce the atrophy-related ubiquitin ligase atrogin-1 and cause skeletal muscle atrophy. *Cell.* 117:399–412. http://dx.doi.org/10.1016/S0092-8674(04)00400-3

Slack, F.J., and G. Ruvkun. 1998. A novel repeat domain that is often associated with RING finger and B-box motifs. *Trends Biochem. Sci.* 23:474–475. http://dx.doi.org/10.1016/S0968-0004(98)01299-7

Solomon, V., and A.L. Goldberg. 1996. Importance of the ATP-ubiquitin-proteasome pathway in the degradation of soluble and myofibrillar proteins in rabbit muscle extracts. *J. Biol. Chem.* 271:26690–26697. http://dx.doi.org/10.1074/jbc.271.41.25240

Tidball, J.G., and M.J. Spencer. 2002. Expression of a calpastatin transgene slows muscle wasting and obviates changes in myosin isoform expression during murine muscle disuse. *J. Physiol.* 545:819–828. http://dx.doi.org/10.1113/jphysiol.2002.024935

Wyke, S.M., and M.J. Tisdale. 2006. Induction of protein degradation in skeletal muscle by a phorbol ester involves upregulation of the ubiquitin-proteasome proteolytic pathway. *Life Sci.* 78:2898–2910. http://dx.doi.org/10.1016/j.lfs.2005.11.014

Yokota, T., M. Mishra, H. Akatsu, Y. Tani, T. Miyauchi, T. Yamamoto, K. Kosaka, Y. Nagai, T. Sawada, and K. Heese. 2006. Brain site-specific gene expression analysis in Alzheimer's disease patients. *Eur. J. Clin. Invest.* 36:820–830. http://dx.doi.org/10.1111/j.1365-2362.2006.01722.x

Zhao, J., J.J. Brault, A. Schild, P. Cao, M. Sandri, S. Schiaffino, S.H. Lecker, and A.L. Goldberg. 2007. FoxO3 coordinately activates protein degradation by the autophagic/lysosomal and proteasomal pathways in atrophying muscle cells. *Cell Metab.* 6:472–483. http://dx.doi.org/10.1016/j.cmet.2007.11.004

Zhao, J., J.J. Brault, A. Schild, and A.L. Goldberg. 2008. Coordinate activation of autophagy and the proteasome pathway by FoxO transcription factor. *Autophagy*. 4:378–380.